Bull. Mater. Sci., Vol. 23, No. 5, October 2000, pp. 345–348. © Indian Academy of Sciences.

Solid-state synthesis and characterization of $LiCoO_2$ and $LiNi_yCo_{1-y}O_2$ solid solutions

P PERIASAMY*, B RAMESH BABU, R THIRUNAKARAN, N KALAISELVI, T PREM KUMAR, N G RENGANATHAN, M RAGHAVAN and N MUNIYANDI

Advanced Batteries Division, Central Electrochemical Research Institute, Karaikudi 630 006, India

MS received 30 June 2000; revised 14 August 2000

Abstract. Solid solutions of compositions $LiNi_yCo_{1-y}O_2$ (y = 0·0, 0·1 and 0·2) were prepared by solid-state fusion synthesis from carbonate precursors. Material characterization was carried out using XRD. Formation mechanisms of the products are discussed in the light of TG/DTA results. Nickel-containing compositions gave higher discharge capacities and smaller hystereses in their charge–discharge profiles which make them more attractive than pristine $LiCoO_2$ as cathode materials in high-energy lithium cells. The lower loss in capacity per cycle for cells with unsubstituted $LiCoO_2$, as determined from cycling studies up to 25 cycles, makes it more suitable than the substituted ones for long cycle-life cells with low capacity fade.

Keywords. Lithium-ion cells; nickel doped $LiCoO_2$; lithium cobalt oxide.

1. Introduction

Ternary layered oxides of the α-$NaFeO_2$ ($R3m$) structure such as $LiCoO_2$ and $LiNiO_2$ have been of much interest as cathode active materials in rechargeable lithium batteries. To take advantage of the low cost and reduced toxicity of nickel while at the same time retain the structural stability of $LiCoO_2$, several groups have investigated isostructural nickel doped $LiCoO_2$. Such solid solutions of the general formula $LiNi_yCo_{1-y}O_2$ have practical reversible capacities of over 150 mAh/g (Heider *et al* 1998) and exhibit lower insertion potentials compared to the pure $LiCoO_2$ phase. Thus $LiNi_yCo_{1-y}O_2$ solid solutions are expected to be oxidatively less taxing on the electrolyte than $LiCoO_2$ and to possibly retain good lamellar structure upon repeated cycling (Delmas and Saadoune 1992; Delmas *et al* 1993; Ohzuku *et al* 1993; Saadoune and Delmas 1996). In the present study we compare the physicochemical characteristics and electrochemical charge–discharge behaviour of $LiNi_yCo_{1-y}O_2$ (y = 0·0, 0·1 and 0·2) obtained by solid state fusion synthesis from carbonate precursors.

2. Experimental

2.1 *Cathode preparation*

Cathode active materials were prepared by a solid-state fusion method from carbonate precursors as described elsewhere (Ramesh Babu *et al* 2000). For the preparation of the electrodes, the required oxide powder was mixed well with 5% poly (vinylidene fluoride) and 10% acetylene black in N-methyl-2-pyrrolidone to form a slurry. The slurry was then brush-coated on an aluminium foil substrate and dried in an oven at 150ºC for 6 h. Discs of 1·8 cm diameter were punched from these foils so that the loading in the cathode was 0·082 g of the active material. Cathode-limited cells were assembled in an MBraun glove box using standard 2016 coin cell hardware with lithium foil as the anode, 1M $LiAsF_6$ in a 30 : 70 (v/v) mixture of ethylene carbonate and dimethyl carbonate as the electrolyte and Celgard 2400 separator.

2.2 *Material characterization*

Powder X-ray diffraction patterns were recorded on a Jeol JDX 8030 X-ray diffractometer with a nickel-filtered CuK_α radiation. For thermal analytical studies, an STA 1500 simultaneous thermal analysis system of Polymer Laboratories was employed.

3. Results and discussion

3.1 *X-ray diffraction studies*

Typical powder X-ray diffraction patterns of pristine $LiCoO_2$ and $LiNi_yCo_{1-y}O_2$ solid solutions (figures 1 a–c) reveal that all these materials are single phase with the α-$NaFeO_2$ structure, space group $R3m$. This means that Ni^{3+} substitutes isomorphically for Co^{3+} in the solid solu-

*Author for correspondence

tions implying that the lithium ions occupy octahedral sites between $[Ni_yCo_{1-y}O_2]$ infinite slabs formed by edge-sharing $[Ni_yCo_{1-y}O_6]$ octahedra. However, because of the propensity of nickel ions to exchange sites with the lithium ions (Dutta *et al* 1992; Kanno *et al* 1994), it was necessary to look for the existence of cation disorder in the nickel-substituted phases. This cation mixing can be detrimental to the electrochemical performance of the cathode material manifesting itself as diminished rechargeable capacity and poor lithium intercalation properties (Choi *et al* 1998). The ratio of the intensities $I_{(003)}/I_{(104)}$ and/or $I_{(101)}/I_{(102,\,006)}$ are considered to be indicators of cation ordering in these compounds (Dahn *et al* 1990; Morales *et al* 1990). The integrated ratios of the intensity of the (003) peak to that of the (104) peak are 1·33, 1·20 and 1·51 for samples with y = 0·0, 0·1 and 0·2, respectively. This compares well with the results of Fujita *et al* (1997) who report values of 1·13 for $LiNi_{0.85}Co_{0.15}O_2$ prepared in air, 1·49 for $LiNiO_2$ and 1·57 for $LiNi_{0.85}Co_{0.15}O_2$, the latter two compounds prepared in flowing oxygen. For values of less than 1·2 for this ratio, the (108) and (110) peaks or the (006) and (102) peaks become hardly distinguishable. That cation disorder is not present to any significant extent is in agreement with the findings of Julien *et al* (1999) who studied $LiNi_yCo_{1-y}O_2$ solid solutions prepared by sol-gel and combustion processes.

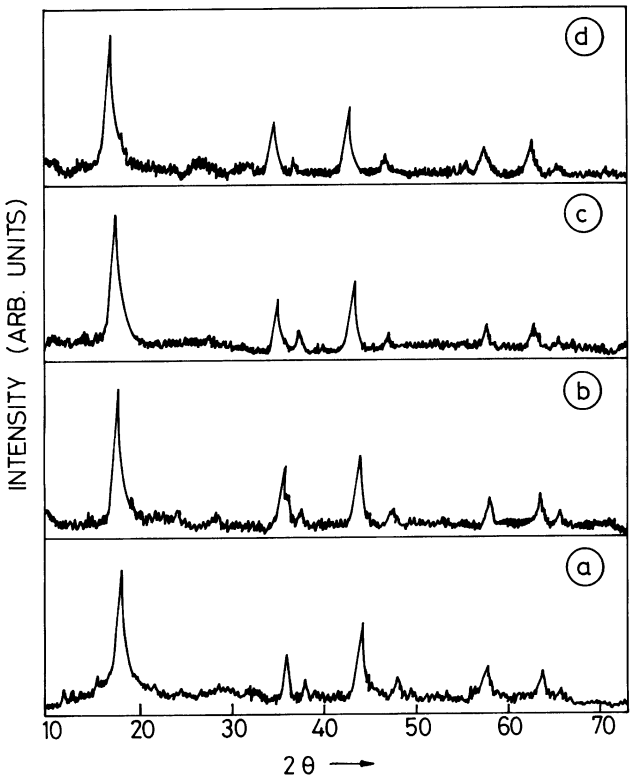

Figure 1. XRD patterns of $LiNi_yCo_{1-y}O_2$ as a function of nickel content. (a) y = 0·0; (b) y = 0·1 and (c) y = 0·2.

3.2 *Thermal analysis*

TG/DTA curves recorded with the carbonate precursors in the stoichiometric ratios corresponding to y = 0·0, 0·1 and 0·2 are presented in figures 2 a–c, respectively. Two regions, a low-temperature region (up to 300ºC) followed by a high-temperature region (up to 800ºC) may be discerned from the thermal profiles. The decomposition patterns of the precursors show no significant change despite changes in the Ni/Co ratio in the precursors. The exothermic peak between 250 and 300ºC may be attributed to a reaction between Li_2CO_3 and $CoCO_3$ in air (Lundbald and Bergman 1997). However, investigations of the decomposition patterns of $CoCO_3$ and Li_2CO_3 in air show that $CoCO_3$ undergoes an endothermic reaction around 270–280ºC to yield Co_3O_4 (Ahmed *et al* 1990; Lundbald

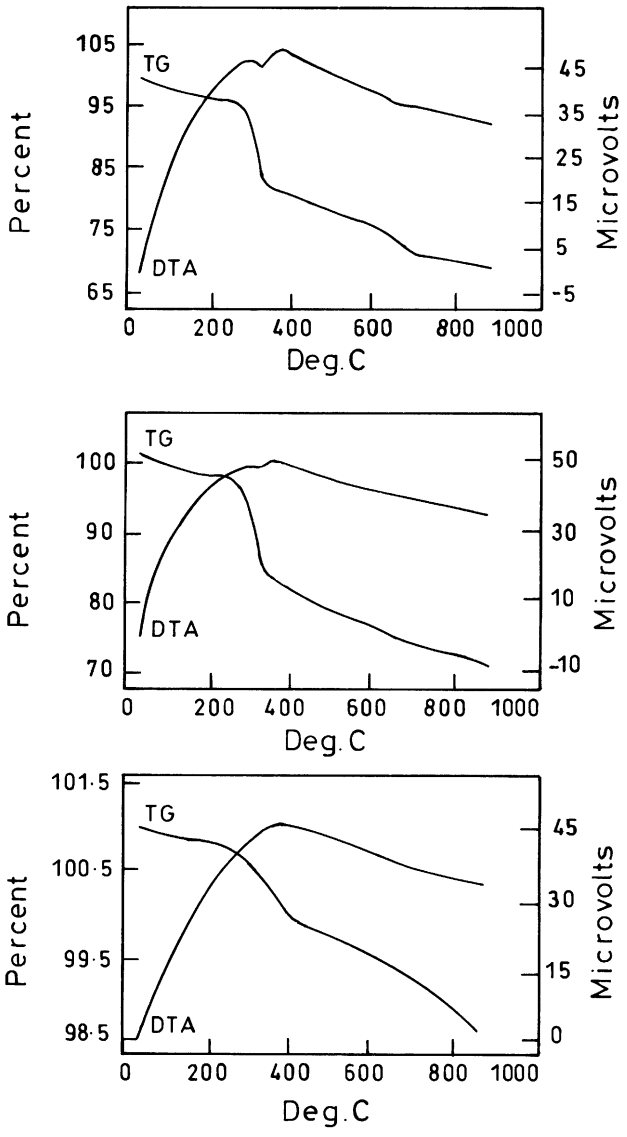

Figure 2. TG/DTA curves of the precursors for $LiCoO_2$, $LiNi_{0.1}Co_{0.9}O_2$ and $LiNi_{0.2}Co_{0.8}O_2$.

and Bergman 1997) and that Li_2CO_3 is stable in air up to 750ºC with a melting point of 723ºC (Lide 1993–1994). The exothermic peak that we have observed may thus be attributed to a possible reaction between the finely divided Co_3O_4 and Li_2CO_3 to form Co_3O_4 with interstitial Li_2O (Lundbald and Bergman 1997). The results are not unexpected given the fact that several carbonates upon mixing produce easily decomposable mixtures (Malik *et al* 1985). Carbon dioxide, a product of the decomposition reaction, in the reaction zone is believed to trigger the melting of an eutectic of composition Li_2CO_3–Li_2O–LiOH around 410ºC (Reisman 1958; Smirnov *et al* 1971). The nickel carbonate hydrate present in the precursors decomposes at 140ºC to the basic carbonate which subsequently loses carbon dioxide and water to produce NiO (Snell and Ettre 1972). The high-temperature region leading to the formation of the final products is supposed to account for the reaction between Li_2CO_3 and Co_3O_4 or Li_2CO_3 and the Co_3O_4 in the interstitials of Li_2O. It must, however, be mentioned here that Co_3O_4 and Li_2O could also react to form $LiCoO_2$ although the formation of the latter has been demonstrated to occur at temperatures as low as 400ºC (e.g. Barboux *et al* 1991). The high temperature region is also supposed to support the reaction of NiO with Li_2CO_3 to give $LiNiO_2$.

3.3 *Charge–discharge studies*

The first charging curves corresponding to the delithiation of $LiNi_yCo_{1-y}O_2$ are shown in figure 3. Delithiation was limited to an upper cut-off voltage of 4·2 V so as not to effect decomposition of the electrolyte. It can be seen that as y increases, the plateau region in the curves shifts to lower voltages. This shift may be ascribed to the contribution made by the Ni^{4+}/Ni^{3+} couple to the cell capacity. For all nickel-containing cathodes, a slight change in the slope of the discharge profiles in the 3·5 to 3·8 V region is discernible, the slope change becoming more pronounced as the nickel content increases. The change in slope indicates two redox processes occurring one after the other. Further, the domain of slope change shifts to the lower potential region as the nickel content is increased. Thus one should expect the oxidation of Ni^{3+} to precede that of Co^{3+} in $LiNi_yCo_{1-y}O_2$. Saadoune and Delmas (1996) and Alcantara *et al* (1995) have demonstrated the preferential oxidation of Ni^{3+} in $LiNi_yCo_{1-y}O_2$ upon electrochemical deintercalation. The lithium intercalation–deintercalation process may thus be represented as a two-step process:

$$Li[Ni_y^{3+}\,Co_{1-y}^{3+}]O_2 \Leftrightarrow$$

$$\square_y Li_{1-y}[Ni_y^{4+}\,Co_{1-y}^{3+}]O_2 + y\,Li^+ + ye^- \Leftrightarrow$$

$$\square_x Li_{1-x}[Ni_y^{4+}\,Co_{x-y}^{4+}Co_{1-x}^{3+}]O_2 + (x-y)\,Li^+ + (x-y)e^-.$$

From figure 4 it can be seen that for $LiCoO_2$ the specific charge and discharge capacities in the first cycle were 146 and 132 mAh, respectively, between 3·0 and 4·2 V. The corresponding values for $LiNi_{0.1}Co_{0.9}O_2$ were 150 and 135 mAh, and those for $LiNi_{0.2}Co_{0.8}O_2$ were 153 and 139 mAh. In the twentyfifth cycle, the values dropped to 126 and 118 mAh for $LiCoO_2$. The corresponding values for $LiNi_{0.1}Co_{0.9}O_2$ were 129 and 120 mAh while those for $LiNi_{0.2}Co_{0.8}O_2$ were 130 and 122 mAh. It can thus be seen that the capacity fade per cycle increases with increasing nickel content. It is typically 0·42 mAh/cycle for y = 0·0, 0·49 for y = 0·1 and 0·81 for y = 0·2. The average voltages recorded were as follows: 3·85 V (y = 0·0), 3·80 V (y = 0·1) and 3·74 V (y = 0·2). Figure 4 further shows the reduced hysteresis in the charge–discharge profiles of $LiNi_{0.2}Co_{0.8}O_2$ as compared to that for $LiCoO_2$. In fact, the hysteresis becomes less pronounced as the nickel content is increased. The reduced hysteresis makes nickel-rich cathodes more suitable materials than pristine $LiCoO_2$ for use in lithium secondary cells.

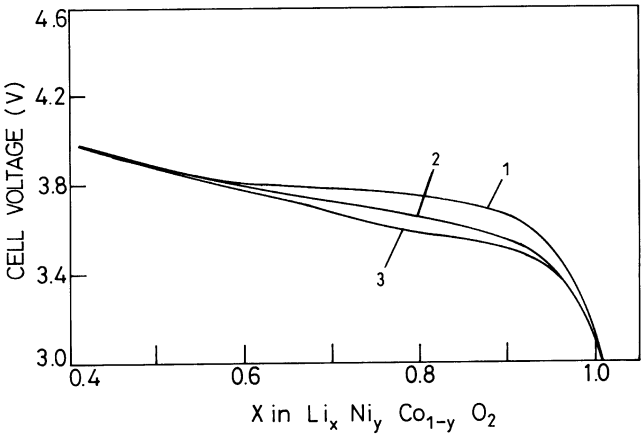

Figure 3. The first charging curves of $Li/LiNi_yCo_{1-y}O_2$ cells. (1) y = 0·0; (2) y = 0·1 and (3) y = 0·2. Charging current: 50 IA.

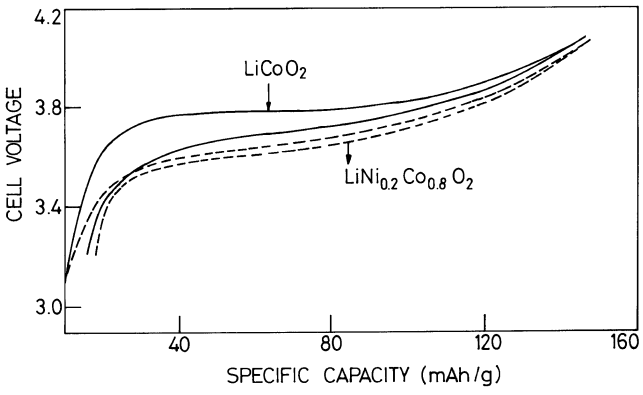

Figure 4. Charge–discharge profiles of $Li/LiNi_yCo_{1-y}O_2$ cells in the first and twentyfifth cycles. (1) y = 0·0; (2) y = 0·1 and (3) y = 0·2. Rate: 50 µA.

4. Conclusions

$LiNi_yCo_{1-y}O_2$ solid solutions have been synthesized using solid state fusion method. X-ray diffraction studies show little or no evidence of cation mixing disorder in the compounds. A knee region on the discharge curves of the nickel substituted compounds show that the oxidation of Ni^{3+} precedes that of Co^{3+}. Compared to the pristine $LiCoO_2$, the nickel substituted compounds show not only higher discharge capacities but also smaller hystereses in the charge–discharge profiles. They thus appear to be attractive candidates for cathodes in lithium–ion cells. However, despite its lower discharge capacity, $LiCoO_2$ exhibits reduced fades upon cycling which qualifies it for long cycle-life cells.

References

Ahmed A I, El-Hakam S A and Samra S E 1990 *Indian J. Chem. Sec. A* **29** 470

Alcantara R, Morales J, Tirado J L, Stoyanova R and Zhecheva E 1995 *J. Electrochem. Soc*. **142** 3997

Barboux P, Tarascon J M and Shokoohi F K 1991 *J. Solid State Chem*. **94** 185

Choi Y M, Pyun S I, Moon S I and Hyung S E 1998 *J. Power Sources* **72** 83

Dahn J R, von Sacken U and Michal C A 1990 *Solid State Ionics* **44** 87

Delmas C and Saadoune I 1992 *Solid State Ionics* **53–56** 370

Delmas C, Saadoune I and Rougier A 1993 *J. Power Sources* **43–44** 595

Dutta G, Manthiram A, Goodenough J B and Grenier J -C 1992 *J. Solid State Chem*. **96** 123

Fujita Y, Amine K, Maruta J and Yasuda H 1997 *J. Power Sources* **68** 68

Heider U, Oesten R, Heider L, Niemann M, Amann A and Lotz N 1998 *15th Int. sem. and exhibition on primary and secondary batteries* (Florida)

Julien C, Michael S S and Ziolkiewicz S 1999 *Int. J. Inorg. Mater*. **1** 29

Kanno R, Kubo H, Kawamoto Y, Kamiyama T, Izumi F, Takeda Y and Takano M 1994 *J. Solid State Chem*. **110** 216

Lide D R (ed.) 1993–1994 *Handbook of chemistry and physics* (Ohio: The Chemical Rubber Company Press) 74th ed.

Lundbald A and Bergman B 1997 *Solid State Ionics* **96** 173

Malik W U, Gupta D R, Masood I and Gupta R S 1985 *J. Mater. Sci. Lett*. **4** 532

Morales J, Perez-Vicente C and Tirado J L 1990 *Mater. Res. Bull*. **25** 623

Ohzuku T, Ueda A, Nagayama M, Iwakoshi Y and Komori H 1993 *Electrochim. Acta* **38** 1159

Ramesh Babu B, Periasamy P, Thirunakaran R, Kalaiselvi N, Prem Kumar T, Renganathan N G, Raghavan M and Muniyandi N 2000 *Int. J. Inorg. Mater*. (communicated)

Reisman A 1958 *J. Am. Chem. Soc*. **80** 3558

Saadoune I and Delmas C 1996 *J. Mater. Chem*. **6** 193

Smirnov M V, Lyubimtseva I Ya, Tsiovkina L A and Krasnov Yu N 1971 *Russ. J. Inorg. Chem.* **16** 130

Snell F D and Ettre L S (eds) 1972 *Encyclopaedia of industrial chemical analysis* (New York: Interscience Publishers) **Vol. 16**, p. 342